AD-A148 570 PROPERTIES OF ULTRA-VIOLET CURED POLY(DIEMTHYLSILOXANE)-UREA ACRYLATES(U) WISCONSIN UNIV-MADISON DEPT OF CHEMICAL ENGINEERING X YU ET AL. 1/1

UNCLASSIFIED NOV 84 TR-6 N00014-83-K-0423 F/G 11/9 NL

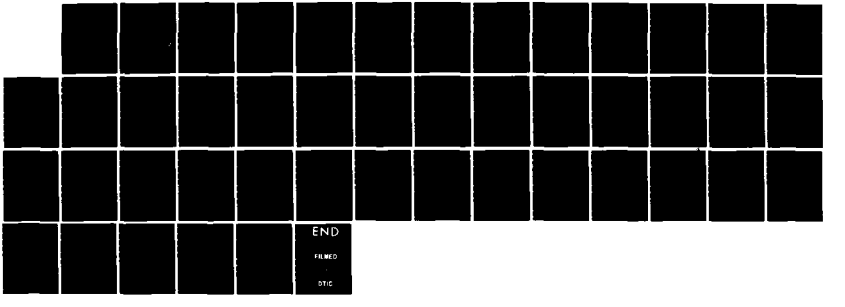

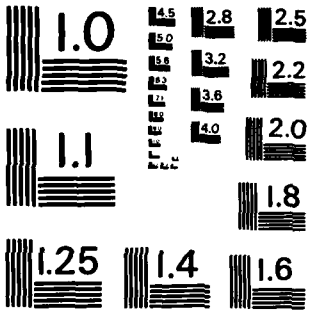

MICROCOPY RESOLUTION TEST CHART
NATIONAL BUREAU OF STANDARDS - 1963 - A

SECURITY CLASSIFICATION

REPORT	READ INSTRUCTIONS BEFORE COMPLETING FORM
1. REPORT NUMBER 6	AD-A148 570 — 3. RECIPIENT'S CATALOG NUMBER
4. TITLE (and Subtitle) Properties of Ultra-Violet Cured Poly(dimethyl-siloxane)-Urea Acrylates	5. TYPE OF REPORT & PERIOD COVERED Interim Technical Report (4)
	6. PERFORMING ORG. REPORT NUMBER
7. AUTHOR(s) X. Yu, M. R. Nagarajan, C. Li, T. A. Speckhard and S. L. Cooper	8. CONTRACT OR GRANT NUMBER(s) N00014-83-K-0423
9. PERFORMING ORGANIZATION NAME AND ADDRESS Department of Chemical Engineering University of Wisconsin Madison, WI 53706	10. PROGRAM ELEMENT, PROJECT, TASK AREA & WORK UNIT NUMBERS
11. CONTROLLING OFFICE NAME AND ADDRESS Department of the Navy Office of Naval Research Arlington, Virginia 22217	12. REPORT DATE Nov. 1, 1984
	13. NUMBER OF PAGES 22
14. MONITORING AGENCY NAME & ADDRESS(if different from Controlling Office)	15. SECURITY CLASS. (of this report) Unclassified
	15a. DECLASSIFICATION/DOWNGRADING SCHEDULE

16. DISTRIBUTION STATEMENT (of this Report)

Distribution unlimited

17. DISTRIBUTION STATEMENT (of the abstract entered in Block 20, if different from Report)

DEC 7 1984

A

18. SUPPLEMENTARY NOTES

To be published in Journal of Applied Polymer Science

19. KEY WORDS (Continue on reverse side if necessary and identify by block number)

Polydimethylsiloxane, acrylate, ultra-violet cured urea

20. ABSTRACT (Continue on reverse side if necessary and identify by block number)

A series of poly(dimethylsiloxane)-urea acrylate prepolymers was synthesized by reacting aminopropyl terminated poly(dimethylsiloxane) (ATPS) with isocyanatoethyl methacrylate (IEM). The oligomers were cured using ultraviolet radiation in the presence of different reactive diluents. Three systems were prepared with varying ATPS soft segment molecular weight. All of the samples were transparent. However, microphase separation was indicated by the observation of two glass transition temperatures attributed to separate ATPS and IEM/reactive

Cont.

DTIC FILE COPY

DD FORM 1 JAN 73 1473 EDITION OF 1 NOV 65 IS OBSOLETE

S/N 0102-LF-014-6601

SECURITY CLASSIFICATION OF THIS PAGE (When Data Entered)

20. Abstract (cont.)

diluent phases. Increasing ATPS molecular weight led to a lower rubbery phase transition temperature and a smaller rigid phase volume fraction. These effects were reflected in lower modulus and tensile strength at room temperature, and higher elongation at break. An increase in the reactive diluent content resulted in an increase in Young's modulus and the ultimate tensile strength of these materials. Increasing reactive diluent content caused the rubbery phase transition peak to decrease in magnitude without changing its position and shifted the hard segment transition to higher temperature. The tensile strengths and moduli of these materials were higher than those reported in the literature for other poly(dimethylsiloxane) and urethane acrylate materials.

OFFICE OF NAVAL RESEARCH

Contract N00014-83-K-0423

TECHNICAL REPORT NO. 6

Properties of Ultra-Violet Cured Poly(dimethylsiloxane)-Urea Acrylates

by

X. Yu, M. R. Nagarajan, C. Li, T. A. Speckhard

and S. L. Cooper

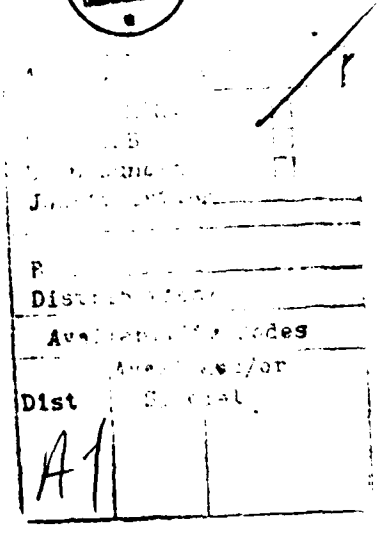

Prepared for Publication

in the

Journal of Applied Polymer Science

Department of Chemical Engineering
University of Wisconsin
Madison, Wisconsin 53706

November 1984

I. INTRODUCTION

High intensity radiation from electron beams or ultraviolet (UV) sources has been shown to be an effective way to initiate polymerization in reactive oligomer systems (1-5). Compared to solvent based systems the advantages of this technology include higher throughput, savings in energy and reduced or eliminated solvent emissions since most formulations are 100% reactive oligomeric liquids. The essential components of radiation curable systems are the reactive oligomer, reactive diluent or comonomer, and photoinitiator. In general, a reactive mixture of oligomer tipped with acrylic functionality is combined with vinyl monomers (reactive diluents) which are added to make harder products and/or to reduce the viscosity of the precursor liquid to obtain better processability. Other components often used in these systems include non-reactive modifiers, pigments, flow control additives and plasticizers.

UV irradiation-induced polymerization is accomplished by the incorporation of suitable ketone-type initiators, usually in combination with accelerators or proton donors (6,7). Such an initiator system produces free radicals upon exposure to light of appropriate wavelength. This technology is now widely used in the printing industry and in coating applications. The most important of the components in determining the mechanical properties of the radiation curable system is the reactive oligomer (2). Therefore, the synthesis of radiation sensitive oligomers has been of considerable interest in recent years (8-17).

Among commercially important radiation curable systems, acrylated urethanes are often employed as oligomers because these materials combine the high abrasion resistance, toughness, tear strength and good low

temperature properties of polyurethanes with the superior optical properties and weatherability of polyacrylates. Commercial urethane acrylate oligomers are normally prepared in a two step procedure by sequentially tipping a difunctional polyether or polyester macroglycol (or polyol) with an aromatic diisocyanate and a hydroxy acrylate such as hydroxyethyl acrylate (HEA). It is also possible to first react the diisocyanate with HEA (or other hydroxy acrylate) and then tip the polyol with that adduct (11). The oligomer may also be functionalized in a one step reaction using isocyanatoethyl methacrylate (IEM) (12,13,18).

In previous publications from this laboratory (11-13) the properties of UV-cured urethane acrylates based on various diisocyanates, hydroxy acrylates, and reactive diluents have been investigated. In an initial study, Koshiba et al. (11) studied the effects of polyol type and molecular weight, diisocyanate type, and reactive diluent content on the properties of UV-cured urethane acrylates. These systems were based on either toluene diisocyanate (TDI) or isophorone diisocyanate (IPDI), HEA, and polycaprolactone or polytetramethylene oxide polyol. In a subsequent publication (12) several families of UV-cured urethane acrylates based on IEM were synthesized and the effects of different polyols (polytetramethylene oxide, polypropylene oxide, polycarbonate, and polycaprolactone) and polyol molecular weight on physical properties were evaluated. TDI/hydroxyethyl methacrylate (HEMA) based samples were also studied and compared to corresponding IEM based materials. The effects of reactive diluent content and type (N-vinyl pyrrolidone (NVP), and di-, tri-, or tetramethylene glycol diacrylate) on the properties of various IEM and TDI/HEMA based materials have also been investigated (13).

Among thermosetting polymers which are processable in the liquid state and used as casting resins in various engineering applications, crosslinked poly(dimethylsiloxanes) are of special interest (19-23). They exhibit many useful properties, such as resistance to temperature extremes, inertness to environmental effects, outstanding dielectric characteristics, high oxygen permeability and unusual surface properties. Disadvantages of these materials include the fact that they are mechanically weak, sensitive to non-polar fluids and demonstrate poor adhesion to substrates.

Only a few publications (24-27) have appeared describing the UV-curing of poly(dimethylsiloxane)-acrylates in detail. Katz and Zewi (24-26) have investigated the effects of phase separation on UV-cured crosslinked poly(dimethylsiloxanes). The occurrence of multiple transitions in the modulus versus temperature curves was ascribed to phase separation. They suggested that microheterogeneities can be expected in crosslinked polymers when the size of the crosslinking site is significant in comparison to the network chain length and when its cohesive energy density differs considerably from that of the primary network chains. Chromecek et al. (27) have investigated the properties of UV-cured α,ω-bis(γ-methacrylic alkyl)-poly(dimethylsiloxane) using iso-bornyl methacrylate as a diluent.

Although the unique properties of crosslinked poly(dimethylsiloxanes) noted above make them desirable candidates for a variety of radiation curable applications, in practice applications are limited due to their poor mechanical properties and their limited miscibility with many reactive diluents. The relatively good mechanical properties of polyurethane acrylates (2,11-17) suggest that incorporation of polar urethane or urea

groups into the siloxane oligomer backbone may result in improved mechanical properties. Insertion of such polar groups may also improve miscibility of the siloxane oligomer with various reactive diluents which in turn may also improve the mechanical properties of the cured siloxane material. However, modification of a siloxane oligomer with urethane or urea groups may also affect the desirable properties of the base polymer.

The present study focuses on the structure-mechanical property relations of radiation sensitive materials based on isocyanatoethyl methacrylate (IEM), amine terminated poly(dimethylsiloxane) (ATPS) and various polar reactive diluents. The reactive diluents or crosslinkers chosen were: ethyl methacrylate (EMA), hydroxyethyl methacrylate (HEMA), butyl acrylate (BA), acrylic acid (AA), methyl methacrylate (MMA), and 4-vinyl pyridine (4VP); their chemical structures are shown in Figure 1. The effects of oligomer (ATPS) molecular weight and reactive diluent type and amount on mechanical properties are investigated in this study using differential scanning calorimetry, dynamic mechanical spectroscopy and stress-strain testing. There are several reasons for choosing this system to study. First, IEM is a monomer which combines both the acrylate and isocyanate functionality into one molecule thus eliminating one step in the oligomer synthesis (18). The chemistry of either functionality may be carried out independently without affecting the latent reactivity of the other group. Secondly, the solubility parameter of the prepolymer is increased when the amine terminated poly(dimethylsiloxane) is reacted with IEM forming a polar urea -NHCONH- linkage in the molecule. This feature increases the compatibility of the oligomer with polar reactive diluents.

II. EXPERIMENTAL

A. Materials

α,ω,-bis(γ-aminopropyl) poly(dimethylsiloxane) (ATPS) was synthesized by coequilibration of octamethylcyclotetrasiloxane (D4) (Petrarch Systems Inc.) and 1,3,bis(γ-aminopropyl)tetramethyldisiloxane (AT) (Silar Laboratories Inc.) using 0.1 wt.% tetramethylammonium hydroxide (Aldrich) as a catalyst at 80°C in a nitrogen atmosphere. After 10 hours, the product was heated to 140-150°C for an hour to decompose the catalyst. Cyclic siloxanes were then removed by vacuum distillation at 130°C (20 mm Hg). Gel permeation chromatography showed no monomer peaks. The molecular weights were determined by titration with hydrochloric acid in isopropyl alcohol using Bromophenol Blue as an indicator.

UV-curable poly(dimethylsiloxane)-urea acrylate oligomers (ATPS-IEM-O) were synthesized (Figure 1a) by slowly adding two moles of isocyanatoethyl methacrylate (IEM) to one mole of ATPS. The IEM was kindly provided by M. R. Thomas of Dow Chemical Company at a purity greater than 99%. The temperature was kept below 45°C to avoid thermal polymerization of the vinyl group. The oligomer was allowed to stand overnight to complete the reaction before curing. Completion of the reaction was confirmed by the disappearance of the NCO peak using Fourier transform infrared spectroscopy (FTIR).

The photoinitiator used was a 1:1 mixture of 2,2'-diethoxyacetophenone (Polysciences) and N-methyldiethanolamine (Aldrich). About 0.6 wt.% of the initiator mixture was added to the oligomer prior to curing. The reactive diluents chosen in this study were: n-butylacrylate (BA), acrylic acid (AA), ethyl methacrylate (EMA), β-hydroxyethyl methacrylate (HEMA), methyl methacrylate (MMA), and 4-vinylpyridine (4-VP).

EMA was obtained from Polysciences and the other reactive diluents were obtained from Aldrich. All the reactive diluents were used as received. The IEM and reactive diluents contained inhibitor to ensure a stable shelf life.

The composition of the UV-curable poly(dimethylsiloxane)-urea acrylate systems was varied in two ways. The molecular weight of the soft segment (ATPS) was varied while the reactive diluent content was kept constant. Secondly, the reactive diluent content was varied at fixed ATPS molecular weight. In total, three families of materials with different ATPS molecular weights comprising 23 samples were studied. A description of each of the materials is given in Table 1. Sample designation codes are based on ATPS molecular weight and reactive diluent content. For example, ATPS-1700-IEM-HEMA20 indicates a 1700 molecular weight ATPS reacted with IEM and cured with 20 wt.% HEMA.

B. Sample Preparation

The mixture of ATPS-IEM, 0.6 wt.% photoinitiator and reactive diluent was poured into an aluminum dish to about 0.2-0.3 mm thickness for tensile testing and .03-.1 mm for dynamic mechanical measurement. The sample was irradiated from one side under a nitrogen atmosphere using a bank of 20W mercury lamps (λ = 365 nm) as the irradiation source. An irradiation time of 30 minutes was found to completely cure the specimens. After UV-curing, all samples were dried in a vacuum oven at 60-70°C for at least 12 hours to remove unreacted reactive diluents. All the samples were transparent to visible light.

C. Characterization Methods

1. Gel Fraction (or Solvent Extraction)

The gel fraction of the cured samples was evaluated by extraction using various solvents (toluene, acetone, and isopropyl alcohol) for 24 hours. The choice of the solvent was dictated by the choice of reactive diluent. The insoluble gel material was dried under vacuum for about two days at 60°C and weighed to determine the gel fraction.

2. Infrared Spectroscopy

The thin polymer films were cast on KBr plates and infrared spectra were taken before and after UV irradiation using a Nicolet 7199 Fourier Transform Infrared Spectrometer. The resolution was 2 cm^{-1}. Changes in the absorption peaks at 1300 cm^{-1} and 910 cm^{-1} assigned to the C=C stretching of acrylates were used to follow the reaction of the vinyl groups.

3. Stress-Strain Measurements

Stress-strain measurements were carried out using a table model Instron tensile testing machine at room temperature with a crosshead speed of 0.254 cm/min. 200 μm thick UV-cured samples were stamped out using an ASTM D1708 die. The dumbbell samples were strained to failure and the engineering stress was calculated as the ratio of force to initial cross-sectional area.

4. Dynamic Mechanical Measurements

Dynamic mechanical data were obtained at 110 Hz using a Toyo Rheovibron dynamic viscoelastomer model DDV-IIC which was controlled automatically by a LSI-11/03 microprocessor. Film samples of about 20×3×0.04 mm in size were tested under a stream of moisture free nitrogen from -150° to 200°C at a heating rate of 2°C/min.

5. Differential Scanning Calorimetry

DSC thermograms of the poly(dimethylsiloxane)-urea acrylate prepolymers and UV-cured polymers were obtained using a Perkin-Elmer DSC-II equipped with a thermal data station. The data was collected from -140° to 200°C at a heating rate of 20°C/min under a helium purge. The DSC thermograms were normalized to equivalent sample weight for comparison.

III. RESULTS AND DISCUSSION

1. Extent of Reaction

Figures 2a-c show the infrared spectra of ATPS-2400 oligomer, and sample ATPS-2400-IEM-0 before and after UV-curing, respectively. A comparison of Figures 2a and 2b shows that reacting IEM with ATPS-2400 results in the formation of urea linkages as indicated by the absorbance peaks at 3300 cm^{-1} (NH) and 1700 cm^{-1} (C=O). The peaks at 1300 cm^{-1} and 910 cm^{-1} in Figure 2b indicate that as expected the acrylate double bond is incorporated into the prepolymer without reacting during the condensation reaction (18). These two peaks disappear after curing (Figure 2c) suggesting that the sample is almost completely crosslinked. The gel fraction data (Table 2) also indicate a nearly complete reaction of the vinyl groups. All of the samples used in this study had gel fractions greater than 95 wt.%.

2. Thermal Analysis

Differential scanning calorimetry (DSC) thermograms for the ATPS-2400-IEM and ATPS-3700-IEM series materials are shown in Figures 3 and 4, respectively. The glass transition temperatures determined from the thermograms are listed in Table 3 along with values for the ATPS-1700-IEM series materials (data not shown). All of the samples exhibit a distinct

glass transition at -110° to -120°C attributable to the poly(dimethylsiloxane) segments. Table 3 shows that at all three ATPS molecular weights there is practically no effect of varying the amount or type of reactive diluent on the glass transition temperature of the poly(dimethylsiloxane) segments. This behavior has been noted previously in urethane acrylate systems (11-13) and was attributed to a high degree of microphase separation of the polyol and urethane acrylate/reactive diluent components. In poorly phase separated urethane acrylate materials, addition of a reactive diluent has been noted to promote the development of a separate urethane acrylate/reactive diluent phase thereby lowering the T_g of the polyol rich phase (13). Alternatively, if the isocyanate and acrylic containing parts of the molecule mix with the polyol segments, changing the reactive diluent type or content will affect the polyol glass transition temperature (13). In light of the large polarity difference between the ATPS and IEM/reactive diluent components and the relatively high molecular weight of the ATPS used in this study, it is reasonable to assume that the constancy of the ATPS T_g is indicative of a high degree of microphase separation between the ATPS and urea acrylate/reactive diluent components of these materials.

The thermograms in Figures 3 and 4, however, do not generally exhibit distinct high temperature glass transitions that can be ascribed to a separate urea acrylate/reactive diluent phase. Similar behavior has been observed in urethane acrylate systems that were determined to be two phase materials by dynamic mechanical spectroscopy (11-13). In general, the low weight fraction of the acrylate/reactive diluent component in the material coupled with a broad transition zone make the detection of the acrylate/

reactive diluent (hard segment) glass transition by DSC difficult. Further evidence for a two phase microstructure in these materials will be presented in the dynamic mechanical data discussed below.

Table 2 shows that the effect of varying the ATPS molecular weight from 1700 to 3700 results in a slight decrease in the poly(dimethylsiloxane) glass transition temperature. This phenomenon is commonly observed in both crosslinked urethane acrylate (12) and phase separated urethane block copolymers (28,29). The crosslink points or the rigid hard segments serve to constrain the mobility of the polyol (soft) segments resulting in a higher T_g than that exhibited by the pure polyol oligomer. As the length of the soft segments increases the effect becomes proportionately less and T_g decreases so as to approach the pure soft segment T_g. From a free volume standpoint the monomer units in the middle of the soft segment chains have greater free volume than those connected to the hard segments. In the case of pure oligomers the trend observed is one of decreasing T_g with decreasing molecular weight since the effect of the free chain ends is to increase the free volume of the system.

3. Mechanical Properties

Stress-strain curves for several different families of materials are shown in Figures 5, 7, 10 and 13, while tensile properties of all the samples are compiled in Table 4. Dynamic mechanical data are displayed for various series of materials in Figures 6, 8, 9, 11, 12, and 14 with transition temperature data listed for all the samples in Table 3. The effect of ATPS molecular weight on the tensile properties of the ATPS-2400-IEM-O series materials is shown in Figure 5. Figure 5 and Table 4 reveal that increasing ATPS molecular weight results in increasing elongation

at break but decreasing Young's modulus. An increase in ATPS molecular weight leads to a longer chain length between crosslinks, and this reduction in the crosslink density should give rise to a lower modulus and greater elongation. Figure 6 shows the dynamic mechanical properties of the ATPS-IEM-0 system of materials as a function of ATPS molecular weight. These materials possess two glass transition temperatures which is indicative of microphase separation. Thus, the argument for the existence of phase separation based on the constancy of the soft segment T_g discussed above appears to be verified. In this case, the IEM and ATPS components phase separate and the IEM rich regions exist in a glassy state at room temperature. Therefore, these IEM rich regions serve as a filler and multi-functional crosslinks and increase the room temperature modulus of the material. In this series of samples the weight percent of the IEM component is inversely related to the ATPS molecular weight (see Table 1). Thus, increasing the ATPS molecular weight lowers the modulus by reducing the volume fraction of the IEM rich domains.

Figure 6 also shows that an increase in the ATPS molecular weight causes an increase in magnitude and a shift to lower temperature of the soft segment glass transition. The shift in T_g to lower temperature is in agreement with the DSC data and is attributed to a reduction of the effect of chain restrictions on the ATPS segments as the ATPS segment length increases. The increase in magnitude (size of E" peak or shoulder which is comparable to the size of a peak or shoulder in the tan δ curve) of the glass transition with increasing ATPS molecular weight is ascribed to a higher weight fraction of ATPS segments in the sample. In contrast to the soft segment T_g, the hard segment glass transition shifts slightly to lower temperatures, and the

E" peak decreases in amplitude with increasing ATPS molecular weight. The decrease in amplitude can be accounted for by the decrease in the weight fraction of the urea acrylate hard segments. The shift to lower temperatures is indicative of more phase mixing in the IEM rich domains at lower weight fraction of the IEM component. The latter behavior could be due to poorer domain organization when there are fewer IEM segments in the sample.

Comparison of the tensile properties of the ATPS-IEM-0 series materials (Figure 5) to the ATPS-IEM-EMA20 series materials (Figure 7) reveals that incorporation of 20 wt.% of EMA increases the Young's modulus, elongation, and stress at break of all the samples. This is primarily due to an increase in the hard segment content in the ATPS-IEM-EMA20 series of materials since the EMA is assumed to combine with the IEM groups to form a separate phase. Figure 8 shows the dynamic mechanical properties of the ATPS-IEM-EMA20 series materials. The magnitude of the hard segment glass transition is increased relative to the corresponding samples without EMA (Figure 6) thereby supporting the assumption that the EMA groups reside primarily in the hard segment phase. Comparing Figures 6 and 8 also shows that the modulus at high temperatures becomes lower upon addition of EMA. This behavior suggests that using EMA as a reactive diluent results in a reduction of the crosslink density of the material presumably due to copolymerization with the IEM groups. In general, the addition of mono-functional reactive diluents to acrylate systems has been found to reduce the crosslink density of the sample (2,13,14). Finally, the effects of increasing ATPS molecular weight on the mechanical properties and thermal transitions of the ATPS-IEM-EMA20 series materials follow the same trends noted for the ATPS-IEM-0 series of samples.

Figure 9 shows the dynamic mechanical properties of the ATPS-3700-IEM series materials containing different amounts of MMA as a reactive diluent. With increasing MMA content the soft segment glass transition peak decreases in magnitude without changing its position at -120°C, while the higher temperature glass transition peak associated with the hard segments increases in magnitude and shifts to higher temperatures. These effects can be rationalized by assuming that the MMA is being incorporated into the hard segment (IEM) domains. Adding MMA decreases the weight fraction of soft phase without affecting its composition thereby lowering the magnitude of its glass transition without affecting its position. At the same time, incorporating the MMA component (homopolymer $T_g \equiv 105°C$) into the hard segment domains increases the weight fraction and rigidity of the hard segment regions resulting in an increase in the temperature and magnitude (size of E" peak) of the hard segment glass transition. Increasing the weight fraction and stiffness of the hard segment domains also results in an increase in the toughness and modulus of these two-phase materials, as shown in Figure 10 and Table 4. Figure 10 and Table 4 also show that increasing MMA content results in an increased elongation at break attributed to a decreased crosslink density due to copolymerization of MMA and IEM during the curing reaction.

The tensile properties of the ATPS-3700-IEM series of materials as a function of HEMA and EMA content are also shown in Table 4 and Figure 10. The dynamic mechanical properties of these materials are shown in Figure 11. The general trends in the physical property changes which occur with increasing HEMA and EMA content are similar to those for the ATPS-3700-IEM-MMA system. Comparing the data in Figure 10 and Table 4

reveals that at equivalent weight fraction of the reactive diluent, the strength and modulus of the material are increased in the order HEMA>MMA>EMA. This trend parallels the order of polarity of the reactive diluents suggesting that increased polarity of the reactive diluent leads to a stronger material, presumably due to greater compatibility between the polar IEM groups and the reactive diluent. Note (Figure 1) that this trend is not correlated with the homopolymer T_g values of the reactive diluents (MMA>HEMA>EMA), indicating that specific interactions (such as hydrogen bonding) are probably occurring between IEM and some of the reactive diluents. In this particular case, the hydroxy group of HEMA allows for additional hydrogen bonding in the hard segment domains which could give rise to greater hard segment domain cohesion, thereby resulting in greater strength.

Dynamic mechanical storage modulus and loss factor curves are shown in Figure 12 for a series of ATPS-2400-IEM materials reacted with 10 wt.% of several different reactive diluents. These materials exhibit behavior similar to that discussed previously suggesting that they are phase separated materials in which the reactive diluent is incorporated in the hard segment phase. Figure 12 and Table 3 show that the magnitude of the shift of the hard segment glass transition to higher temperature upon addition of reactive diluent follows the order 4VP>HEMA>BA-AA>EMA>BA. This trend reflects the differences in homopolymer T_g and polarity of the various reactive diluents and is also manifested in the samples' strength and room temperature modulus (Figures 12 and 13, and Table 4). The stiffer and more polar reactive diluents appear to strengthen the material to a greater extent. However, the storage moduli at

high temperatures, above the T_g of the hard segment phase, are roughly the same for all of the materials. This behavior is attributed to the fact that all of the materials have similar reactive diluent contents resulting in similar crosslink densities. This observation also suggests that differences in reactivity among the reactive diluents (leading to different amounts of copolymerization with IEM, which should affect the crosslink density) may not be as important as differences in compatibility with IEM in determining the mechanical properties of the material. Finally, it is interesting to note that the sample containing 1 wt.% of acrylic acid and 8 wt.% butyl acrylate demonstrates a noticeable difference in properties compared to the sample with 9 wt.% butyl acrylate. Apparently the increase in polarity and/or reactivity of acrylic acid relative to butyl acrylate has a dramatic effect on the properties of the sample.

The dynamic mechanical properties of ATPS-2400-IEM with 25 wt.% of three different reactive diluents are shown in Figure 14. The general trends in physical property changes are the same as those for the ATPS-2400-IEM-10 series materials discussed above. The trends in room temperature modulus and strength again reflect the compatibility of the various reactive diluents with IEM.

As mentioned in the Introduction the rationale for incorporating urethane or urea groups into poly(dimethylsiloxane) based acrylate materials was to improve mechanical properties. Thus, it would seem appropriate to compare the mechanical properties reported here with mechanical property data on poly(dimethylsiloxane) acrylates. Unfortunately, there is very little mechanical property data on poly(dimethylsiloxane) acrylates in the literature (24-27). Katz and Zewi (24-26) have presented only shear modulus

data which exhibited multiple transitions ascribed to the development of microphase separation. However, increases in modulus due to microphase separation occurred only at temperatures below 25°C. Chromocek et al. (27) have reported tensile properties for a high molecular weight (~13000) α,ω-bis(γ-methacrylic alkyl)-poly(dimethylsiloxane) material using a mixture of isobornyl acrylate (IBA) and acrylic acid (AA) as a reactive diluent. Unfortunately, the tensile data are reported for samples with varying amounts of adsorbed water. One sample with 2.5 wt.% water, 33.3% IBA and 4.8% AA exhibited a tensile strength of 5.7 MPa, a tensile modulus of 33.4 MPa and an elongation at break of 200%. Comparable samples studied here (Table 4) have higher tensile strength and modulus but lower elongation at break. The other samples studied by Chromocek et al. had higher water contents and much lower tensile strengths and moduli. Thus, it would appear that some improvement in strength and modulus particularly at high temperatures results from incorporation of urethane or urea groups into poly(dimethylsiloxane) acrylates.

Polyurethane acrylate materials based on IEM and various soft segment oligomers (polypropylene oxide, polytetramethylene oxide, polycaprolactone and polycarbonate) have been previously studied in this laboratory (12,13). In comparison with those materials the poly(dimethylsiloxane) based samples of this study exhibit a higher degree of phase separation, generally higher tensile strength and modulus, and lower elongation at break. The higher strength and modulus of the poly(dimethylsiloxane) based materials is particularly interesting since in polyurethane block copolymer systems PDMS based samples have been found (31,32) to have greatly decreased mechanical properties in comparison with conventional polyether or polyester based materials. This apparent anomaly would seem to warrant further study.

IV. SUMMARY

A series of poly(dimethylsiloxane)-urea acrylate prepolymers was synthesized and crosslinked in the presence of various monomers using UV irradiation. Three sets of materials were prepared which differed in soft segment molecular weight and the level and type of reactive diluent added. A systematic study of their structure-property relationship has been accomplished using stress-strain testing, dynamic mechanical measurements and differential scanning calorimetry.

All of the cured samples were transparent, even though they possessed a two-phase morphology as demonstrated by the presence of soft and hard segment glass transition temperatures in the dynamic mechanical test. Increasing molecular weight of the ATPS created a longer chain length between crosslinks and lowered the T_g of the soft segment phase. Increasing the soft segment molecular weight led to a lower hard segment content and thereby lower dynamic and tensile moduli and tensile strength at room temperature. The IEM based samples with zero percent reactive diluent exhibited low extensibility. The addition of the reactive diluents decreased the crosslink density due to copolymerization with IEM and thus elongation at break increased. An increase in the reactive diluent content resulted in an increase in Young's modulus and ultimate tensile strength in these materials. The dynamic and tensile moduli at room temperature were found to increase with various reactive diluents in the order 4VP>HEMA>BA-AA>EMA>BA. This behavior was attributed to both an increasing T_g of the hard domains and a greater compatibility between the more polar reactive diluent and urea acrylate segments. The samples of this study when compared with other poly(dimethylsiloxane) and urethane acrylate

materials discussed in the literature exhibited greater tensile strength and modulus but lower elongation at break.

ACKNOWLEDGEMENT

The authors wish to acknowledge support of this work by the Naval Air Systems Command and the Office of Naval Research. One of the authors (X.Y.) would like to express his thanks for financial support provided by the government of the People's Republic of China.

REFERENCES

1. W. Mareau and N. Viswanathan, ACS Org. Coat. Preprints, 35(1), 108 (1975).

2. C. S. Schmidle, J. Coated Fabrics, 8, 10 (1978).

3. J. V. Crivello, ACS Org. Coat. Preprints, 41, 560 (1979).

4. L. Kushner and R. S. Tu, Modern Plastics, 60(4), 87 (1983).

5. C. Decker, ACS Polym. Matl. Preprints, 49, 32 (1983).

6. U.S. Patent Number 2,993,789 (1961).

7. T. Higuchi, in "Photopolymer" edited by T. Tsunoda (CMC, Tokyo) 1977, p. 137.

8. Nippon Kokai Tokyo Koho 48-43657 (1973) (Japanese Patent).

9. Nippon Kokai Tokyo Koho 46-29525 (1971) (Japanese Patent).

10. U.S. Patent 3,907,865 (1975).

11. M. Koshiba, K. K. S. Hwang, S. K. Foley, D. J. Yarusso and S. L. Cooper, J. Materials Sci., 17, 1447 (1982).

12. S. B. Lin, S. Y. Tsay, T. A. Speckhard, K. K. S. Hwang, J. J. Jezerc and S. L. Cooper, Chem. Engr. Comm., in press.

13. T. A. Speckhard, K. K. S. Hwang, S. B. Lin, S. Y. Tsay, M. Koshiba and S. L. Cooper, J. Appl. Poly. Sci., in press.

14. W. Oraby and W. K. Walsh, J. Applied Poly. Sci., 23, 3227 (1979).

15. W. Oraby and W. K. Walsh, J. Applied Poly. Sci., 23, 3243 (1979).

16. K. Park and G. L. Wilkes, ACS Org. Coat. Preprints, 41, 308 (1979).

17. E. G. Joseph, G. L. Wilkes, and K. Park, ACS Polymer Preprints, 20, 520 (1979).

18. M. R. Thomas, ACS Org. Coat. Preprints, 46, 506 (1982).

19. A. Noshay and J. E. McGrath, "Block Copolymers Overview and Critical Survey", Academic Press (1968).

20. W. Noll, "Chemistry and Technology of Siloxanes", Academic Press, New York (1968).

21. G. L. Gaines, Macromolecules, 14, 208 (1981).

22. A. Braley, J. Macromol. Sci.-Chem., A4, 529 (1970).

23. L. Leduc, L. P. Blanchard, and S. L. Malhotra, J. Macromol. Sci.-Chem., A14, 389 (1980).

24. D. Katz and I. G. Zewi, J. Polym. Sci., Polym. Chem. Ed., 16, 597 (1978).

25. D. Katz and I. G. Zewi, J. Polym. Sci., Polym. Chem. Ed., 13, 645 (1975).

26. D. Katz and I. G. Zewi, J. Polym. Sci., C46, 139 (1974).

27. U.S. Patent Number 4,276,402 (1981).

28. T. A. Speckhard, P. E. Gibson, S. L. Cooper, V. S. C. Chang, and J. P. Kennedy, Polymer, in press.

29. D. Z. Zdrahala, S. L. Hager, R. Gerkin, and F. E. Critchfield, J. Elast. and Plast., 12, 225 (1980).

30. J. Brandrup and E. H. Immergut, eds., Polymer Handbook, John Wiley and Sons, Second Edition (1975), Part III, p. 139.

31. X. Yu, M. R. Nagarajan, T. G. Grasel, P. E. Gibson, and S. L. Cooper, submitted to J. Poly. Sci.-Phys.

32. D. Tyagi, I. Yilgor, G. L. Wilkes, and J. E. McGrath, ACS Polymer Preprints, 24, (2), 39 (1983).

33. J. W. C. Van Bogart, A. Lilaonitkul, L. Lerner, and S. L. Cooper, J. Macromol. Sci.-Phys., B17, 267 (1980).

TABLE 1

Sample Characterization

Sample Designation	Wt.% Reactive Diluent	Wt.% Hard Segment[a]
ATPS-1700-IEM-0	0	15.5
ATPS-1700-IEM-EMA9	9	24.1
ATPS-1700-IEM-EMA20	20	37.4
ATPS-1700-IEM-HEMA9	9	24.1
ATPS-1700-IEM-HEMA20	20	37.4
ATPS-1700-IEM-4VP9	9	24.1
ATPS-2400-IEM-0	0	11.4
ATPS-2400-IEM-EMA9	9	19.5
ATPS-2400-IEM-EMA20	20	29.1
ATPS-2400-IEM-HEMA9	9	19.5
ATPS-2400-IEM-HEMA20	20	29.1
ATPS-2400-IEM-4VP9	9	19.5
ATPS-2400-IEM-BA9	9	19.5
ATPS-2400-IEM-BA20	20	29.1
ATPS-2400-IEM-BA(AA)9[b]	9	19.5
ATPS-3700-IEM-0	0	7.7
ATPS-3700-IEM-EMA9	9	16.1
ATPS-3700-IEM-EMA20	20	26.2
ATPS-3700-IEM-HEMA9	9	16.1
ATPS-3700-IEM-HEMA20	20	26.2
ATPS-3700-IEM-MMA9	9	16.1
ATPS-3700-IEM-MMA33	33	38.5
ATPS-3700-IEM-MMA50	50	53.9

[a] Hard segment is defined as reactive diluent and IEM

[b] BA:AA 9:1 wt. ratio

TABLE 2

Gel fractions of UV cured poly(dimethylsiloxane)-urea acrylates

Sample	Gel Fraction (%)	Solvent
ATPS-1700-IEM-0	98.3	Toluene
ATPS-1700-IEM-EMA9	99.7	Acetone
ATPS-1700-IEM-HEMA20	96.4	Isopropanol
ATPS-1700-IEM-4VP9	98.3	Isopropanol
ATPS-2400-IEM-0	99.0	Toluene
ATPS-2400-IEM-BA20	98.4	Acetone
ATPS-3700-IEM-0	97.1	Toluene
ATPS-3700-IEM-EMA20	97.1	Acetone
ATPS-3700-IEM-HEMA20	95.9	Isopropanol
ATPS-3700-IEM-MMA33	96.5	Acetone
ATPS-3700-IEM-MMA50	97.7	Acetone

TABLE 3

Thermal Transitions of poly(dimethylsiloxane)-urea acrylates

Sample	Glass Transition Temperature (°C) From DSC	From E" Peaks	
	T_{g_1}	T_{g_1}	T_{g_2}
ATPS-1700-IEM-0	-111.5	-115	79
ATPS-1700-IEM-EMA9	-113		
ATPS-1700-IEM-EMA20	-113	-116	92
ATPS-1700-IEM-HEMA9	-113		
ATPS-1700-IEM-HEMA20	-114		
ATPS-1700-IEM-4VP9	-113.5		
ATPS-2400-IEM-0	-115.5	-119	85
ATPS-2400-IEM-EMA9	-115	-120	57
ATPS-2400-IEM-EMA20	-115	-121	67
ATPS-2400-IEM-HEMA9	-115	-121	105
ATPS-2400-IEM-HEMA20	-115.5	-120	112
ATPS-2400-IEM-4VP9	-115	-119	112
ATPS-2400-IEM-BA9	-115	-121	68
ATPS-2400-IEM-BA20	-115	-122	76
ATPS-2400-IEM-BA(AA)9	-115	-122	86
ATPS-3700-IEM-0	-118	-126	87
ATPS-3700-IEM-EMA9	-117	-125	84
ATPS-3700-IEM-EMA20	-117	-125	-
ATPS-3700-IEM-HEMA9	-118	-126	104
ATPS-3700-IEM-HEMA20	-	-128	107
ATPS-3700-IEM-MMA9	-119	-124	110
ATPS-3700-IEM-MMA33	-119	-124	116
ATPS-3700-IEM-MMA50	-119	-124	123

TABLE 4

Tensile properties of UV cured poly(dimethylsiloxane)-urea acrylates

Sample	Ultimate tensile strength MPa	Ultimate elongation %	Young's Modulus MPa
ATPS-1700-IEM-0	4.37	7.4	59.0
ATPS-1700-IEM-EMA9	5.20	5.7	91.2
ATPS-1700-IEM-EMA20	8.07	11.4	115.0
ATPS-1700-IEM-HEMA9	7.02	5.8	123.0
ATPS-1700-IEM-HEMA20	11.87	9.4	189.0
ATPS-1700-IEM-4VP9	3.95	5.7	68.4
ATPS-2400-IEM-0	1.24	10.7	115.0
ATPS-2400-IEM-EMA9	2.01	25.1	14.0
ATPS-2400-IEM-EMA20	2.86	28.5	20.5
ATPS-2400-IEM-HEMA9	2.17	10.8	25.8
ATPS-2400-IEM-HEMA20	7.24	18.3	77.9
ATPS-2400-IEM-4VP9	3.15	15.4	35.8
ATPS-2400-IEM-BA9	TOO SOFT TO TEST		
ATPS-2400-IEM-BA20	0.17	9.4	7.7
ATPS-2400-IEM-BA(AA)9	1.92	12.8	18.2
ATPS-3700-IEM-0	0.86	14.5	6.21
ATPS-3700-IEM-EMA9	1.20	19.4	0.70
ATPS-3700-IEM-EMA20	2.21	28.8	1.23
ATPS-3700-IEM-HEMA9	2.23	23.4	14.70
ATPS-3700-IEM-HEMA20	4.19	20.0	35.30
ATPS-3700-IEM-MMA9	1.11	17.4	7.49
ATPS-3700-IEM-MMA33	2.99	28.5	34.20
ATPS-3700-IEM-MMA50	8.9	58.7	82.50

FIGURE CAPTIONS

Figure 1a Oligomer synthesis

Figure 1b Chemical structure of UV-curable acrylate prepolymers and reactive diluents, and glass transition temperatures of homopolymer reactive diluents (30).

Figure 2 Infrared spectra of (a) ATPS-2400 oligomer, (b) ATPS-2400-IEM-0 before UV-curing and (c) ATPS-2400-IEM-0 after UV-curing.

Figure 3 DSC curves of ATPS-2400-IEM-9 and ATPS-2400-IEM-20 series materials.

Figure 4 DSC curves of ATPS-3700-IEM-9 and ATPS-3700-IEM-20 series materials.

Figure 5 Effect of ATPS molecular weight on the tensile properties of the ATPS-IEM-0 systems.

Figure 6 Effect of ATPS molecular weight on the storage modulus (E') and loss tangent of the ATPS-IEM-0 systems.

Figure 7 Effect of ATPS molecular weight on the tensile properties of the ATPS-IEM-EMA-20 system.

Figure 8 Effect of ATPS molecular weight on the storage modulus (E') and loss tangent of the ATPS-IEM-EMA-20 system.

Figure 9 Effect of MMA content on the dynamic mechanical properties of ATPS-3700-IEM.

Figure 10 Effect of MMA, EMA, and HEMA content on the tensile properties of ATPS-3700-IEM.

Figure 11 Effect of HEMA and EMA content on the storage modulus (E') and loss tangent of ATPS-3700-IEM.

Figure 12 The storage modulus (E') and loss tangent of ATPS-2400-IEM-9 series materials.

Figure 13 Effect of HEMA, EMA, BA, 4VP and BA-AA content on the tensile properties of ATPS-2400-IEM.

Figure 14 The storage modulus (E') and loss tangent of ATPS-2400-IEM-20 series materials.

Figure 1a

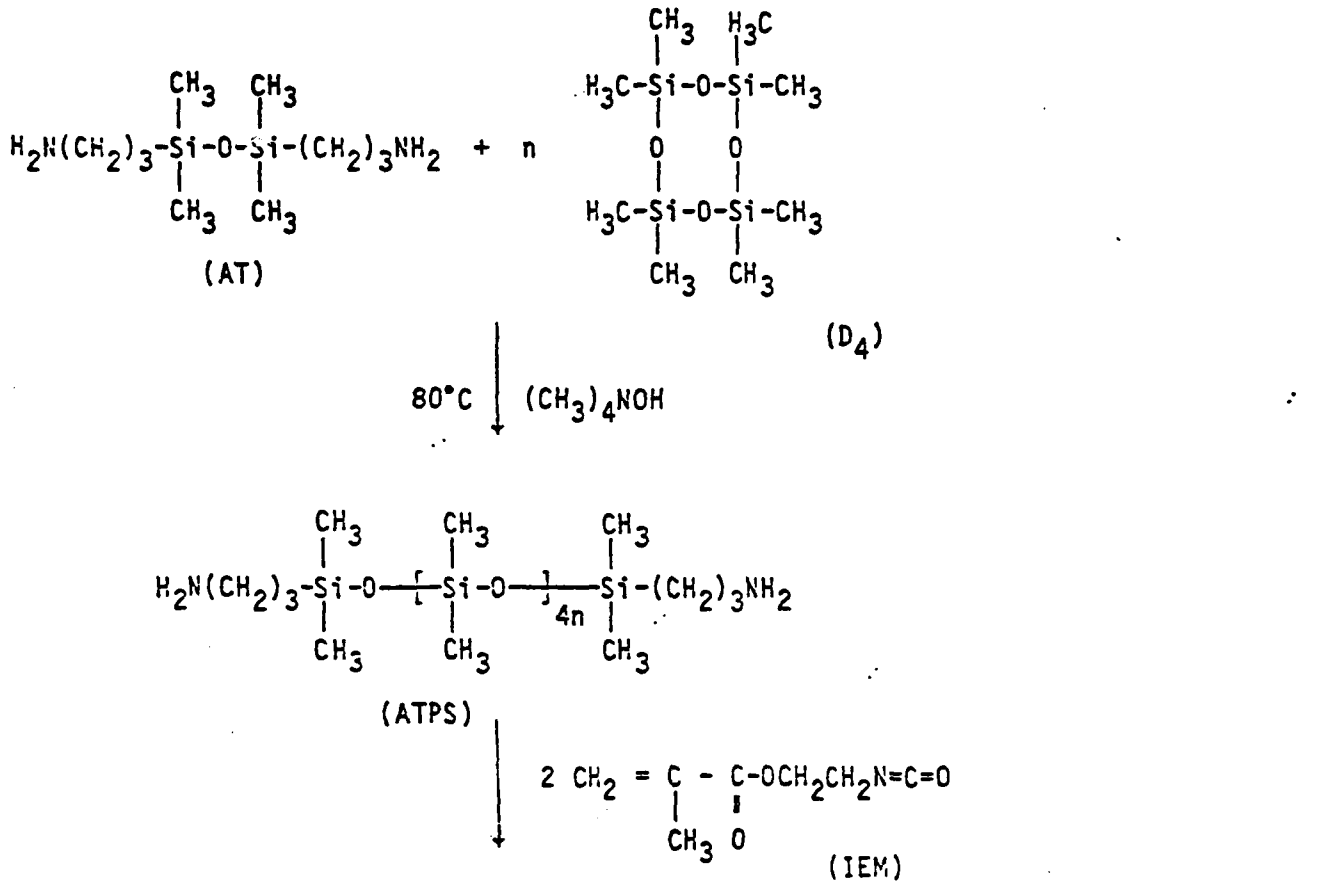

Figure 1b

Reactive diluent structure	Homopolymer T_g (°C) (reference 30)
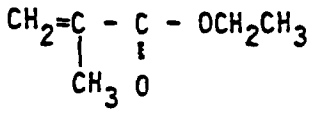	
Ethyl Methacrylate (EMA)	65
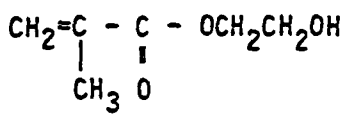	
Hydroxyethyl Methacrylate (HEMA)	86
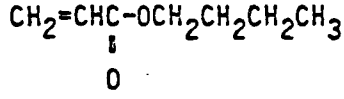	
Butyl Acrylate (BA)	-54
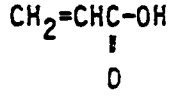	
Acrylic Acid (AA)	-
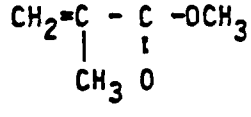	
Methyl Methacrylate (MMA)	105
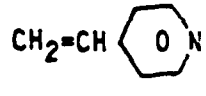	
4N-Vinyl Pyridine (4VP)	140

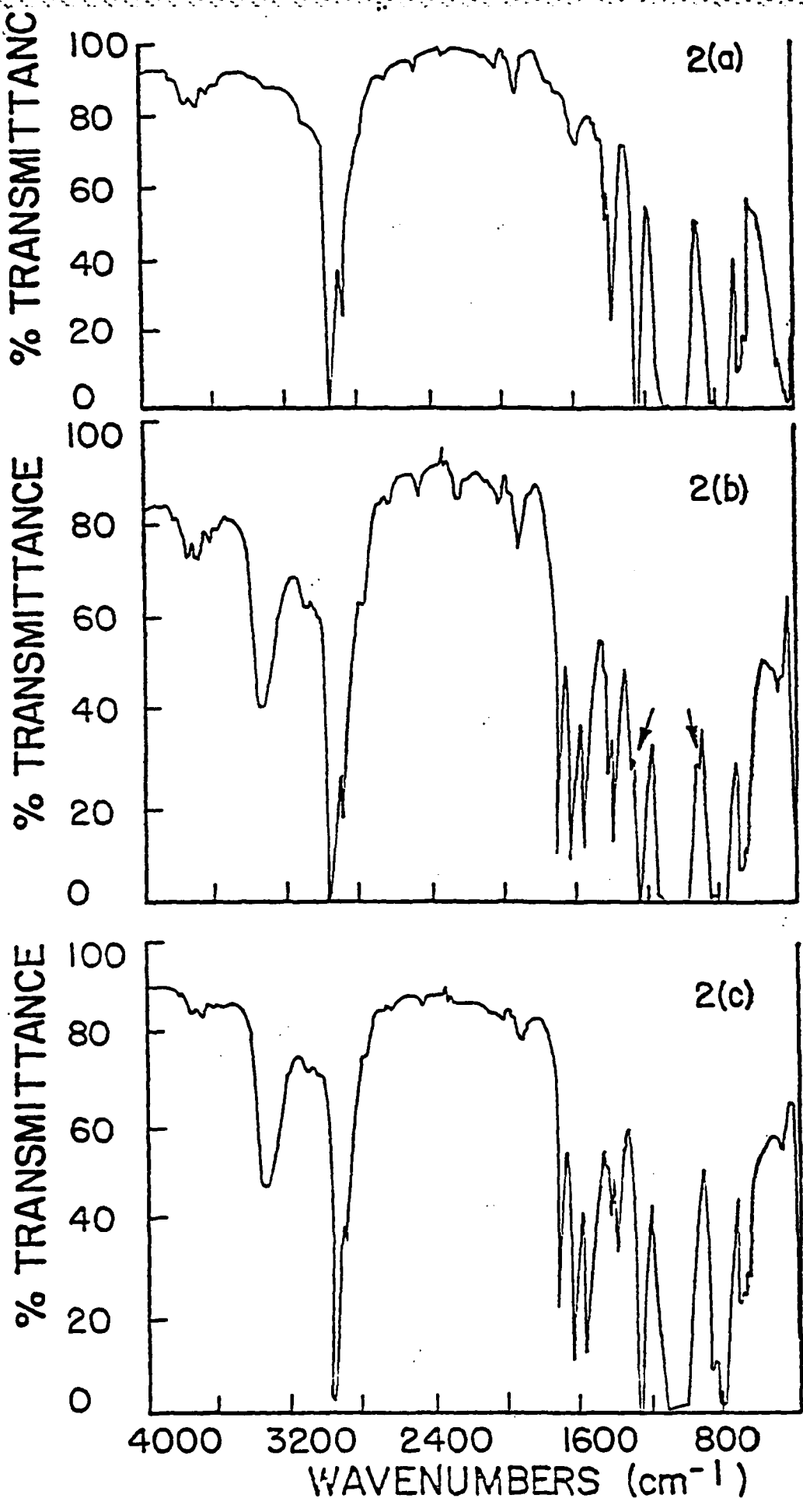
% TRANSMITTANC
100
80
60
40
20
0
2(a)
% TRANSMITTANCE
100
80
60
40
20
0
2(b)
% TRANSMITTANCE
100
80
60
40
20
0
2(c)
4000
3200
2400
1600
800
WAVENUMBERS (cm⁻¹)

FIGURE 2

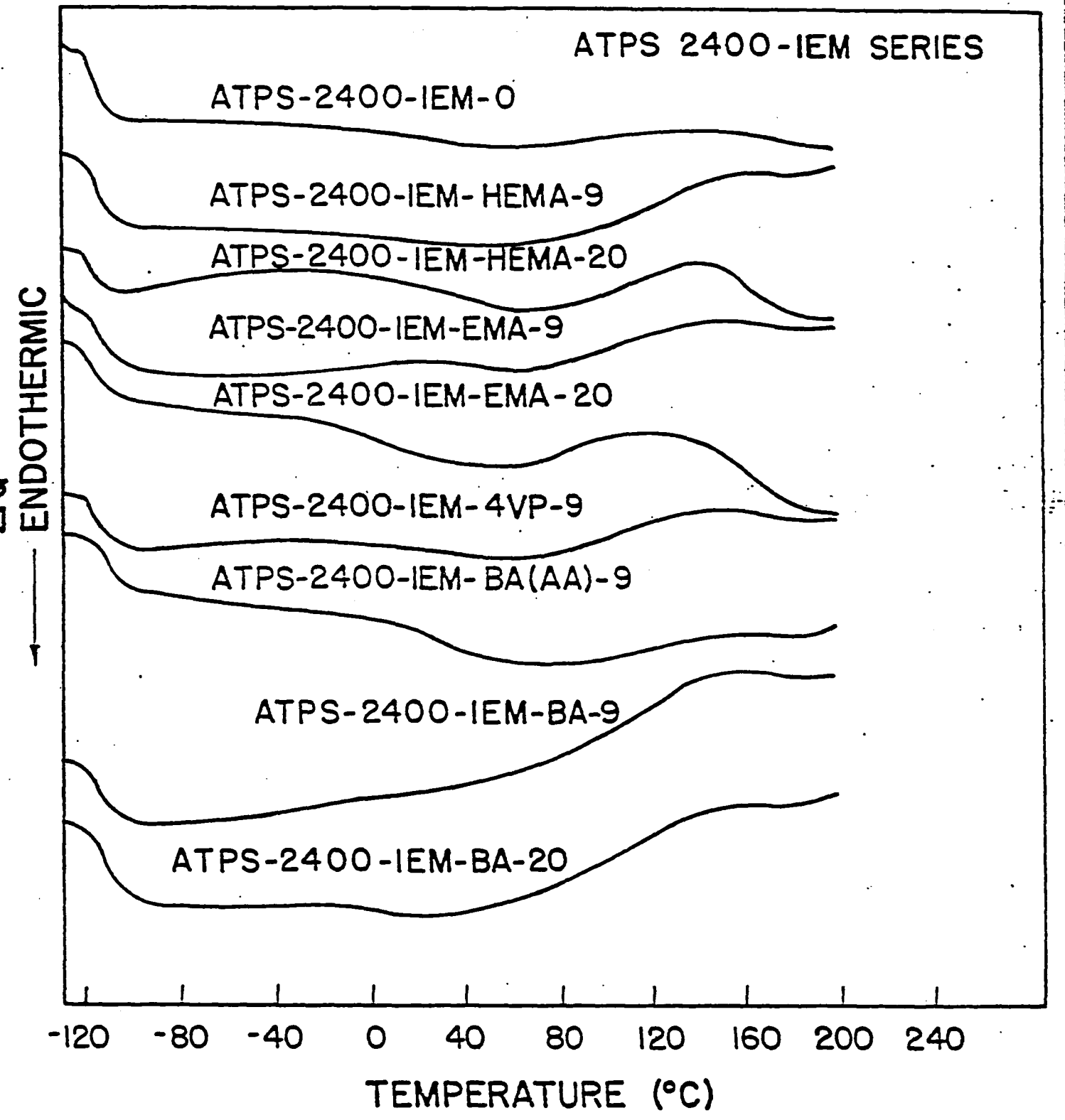
ATPS 2400-IEM SERIES
ATPS-2400-IEM-0
ATPS-2400-IEM-HEMA-9
ATPS-2400-IEM-HEMA-20
ATPS-2400-IEM-EMA-9
ATPS-2400-IEM-EMA-20
ATPS-2400-IEM-4VP-9
ATPS-2400-IEM-BA(AA)-9
ATPS-2400-IEM-BA-9
ATPS-2400-IEM-BA-20
ENDOTHERMIC
-120
-80
-40
0
40
80
120
160
200
240
TEMPERATURE (°C)

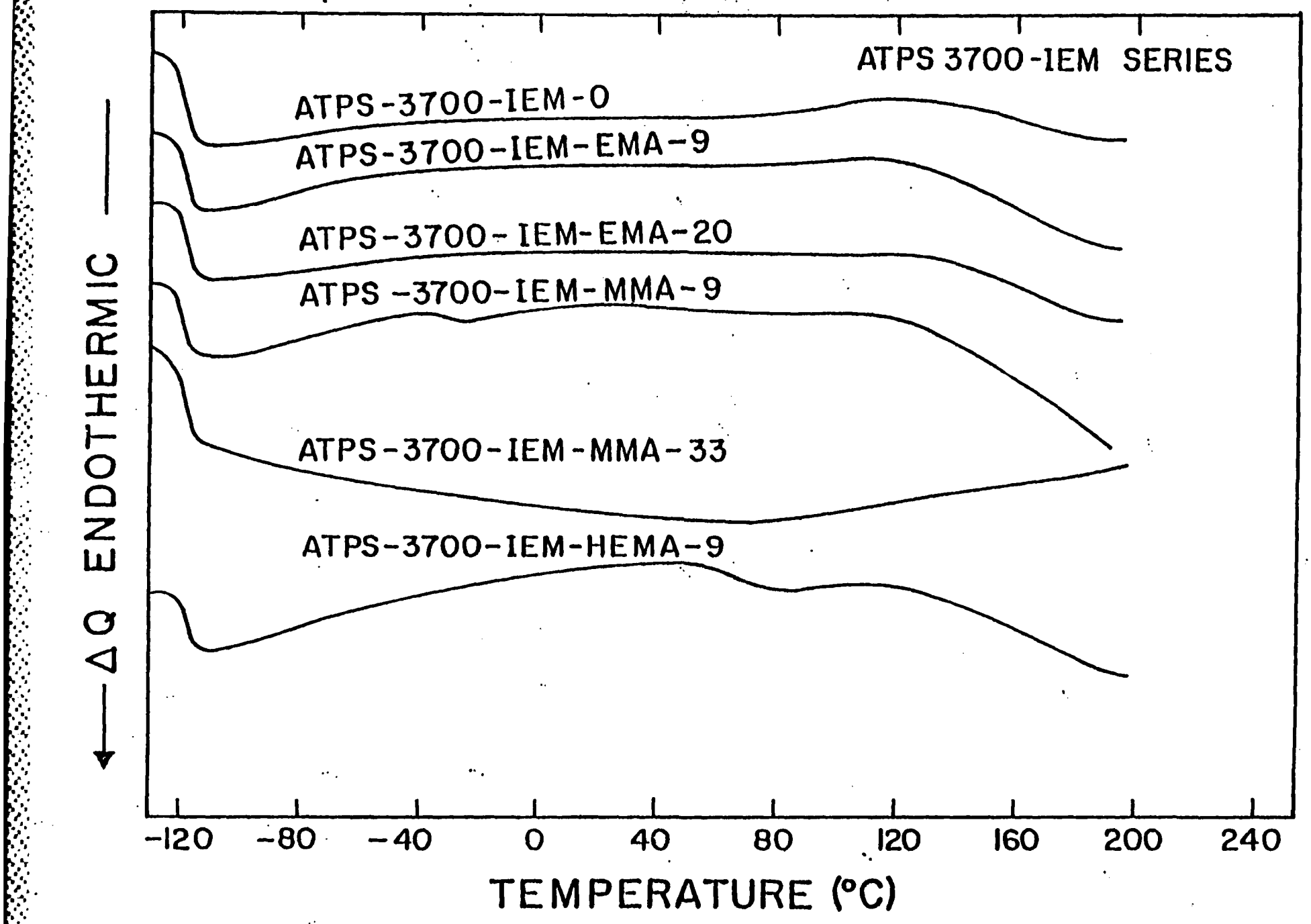
ATPS 3700-IEM SERIES
ATPS-3700-IEM-0
ATPS-3700-IEM-EMA-9
ATPS-3700-IEM-EMA-20
ATPS-3700-IEM-MMA-9
ATPS-3700-IEM-MMA-33
ATPS-3700-IEM-HEMA-9
ΔQ ENDOTHERMIC
-120
-80
-40
0
40
80
120
160
200
240
TEMPERATURE (°C)

FIGURE 4

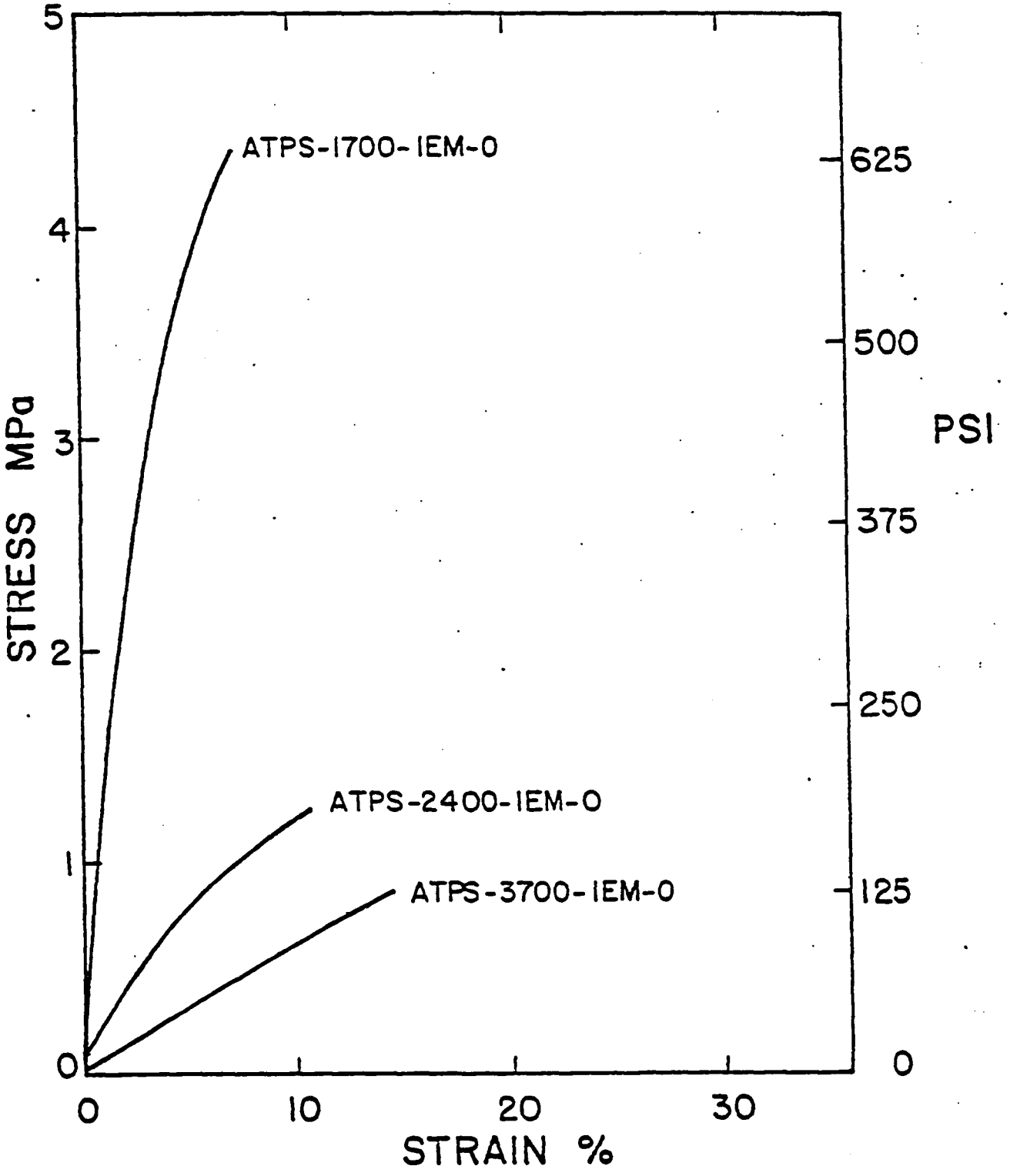
ATPS-1700-1EM-0
ATPS-2400-1EM-0
ATPS-3700-1EM-0
STRESS MPa
PSI
STRAIN %
0
1
2
3
4
5
0
125
250
375
500
625
0
10
20
30

FIGURE 5

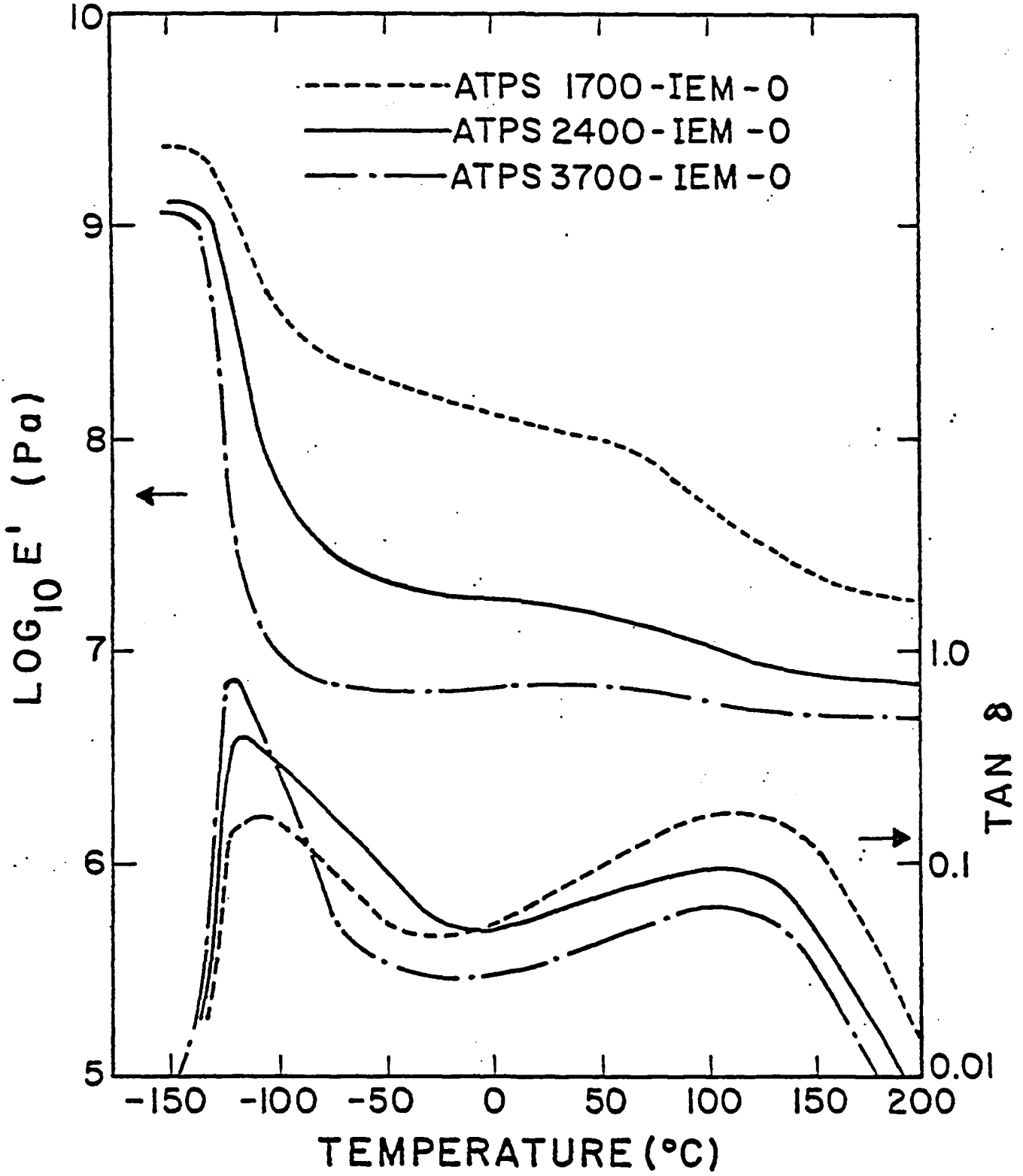
ATPS 1700-IEM-0
ATPS 2400-IEM-0
ATPS 3700-IEM-0
LOG10 E' (Pa)
TAN δ
TEMPERATURE (°C)
10
9
8
7
6
5
1.0
0.1
0.01
-150
-100
-50
0
50
100
150
200

FIGURE 6

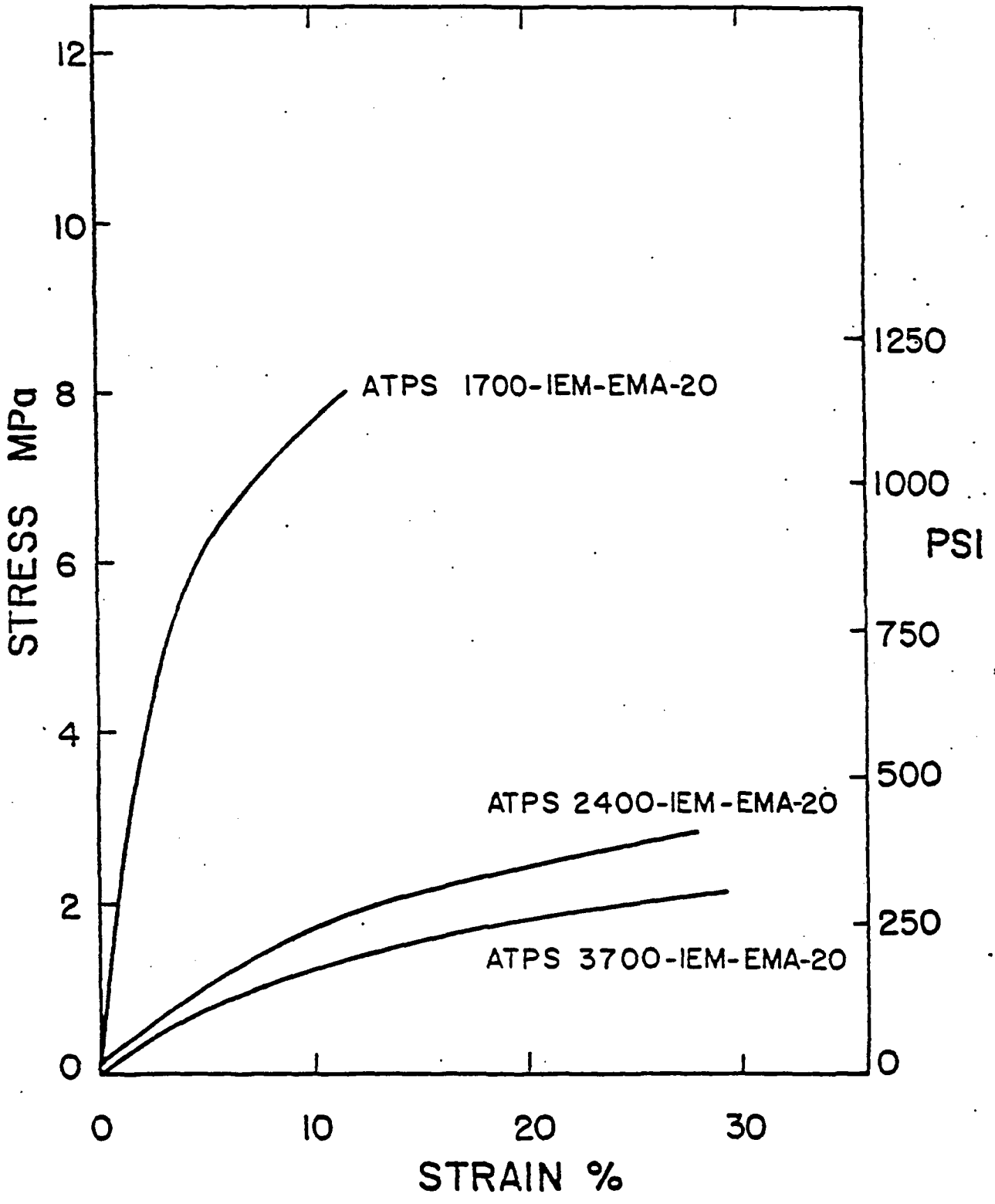
STRESS MPa
12
10
8
6
4
2
0
1250
1000
750
500
250
0
PSI
ATPS 1700-IEM-EMA-20
ATPS 2400-IEM-EMA-20
ATPS 3700-IEM-EMA-20
0
10
20
30
STRAIN %

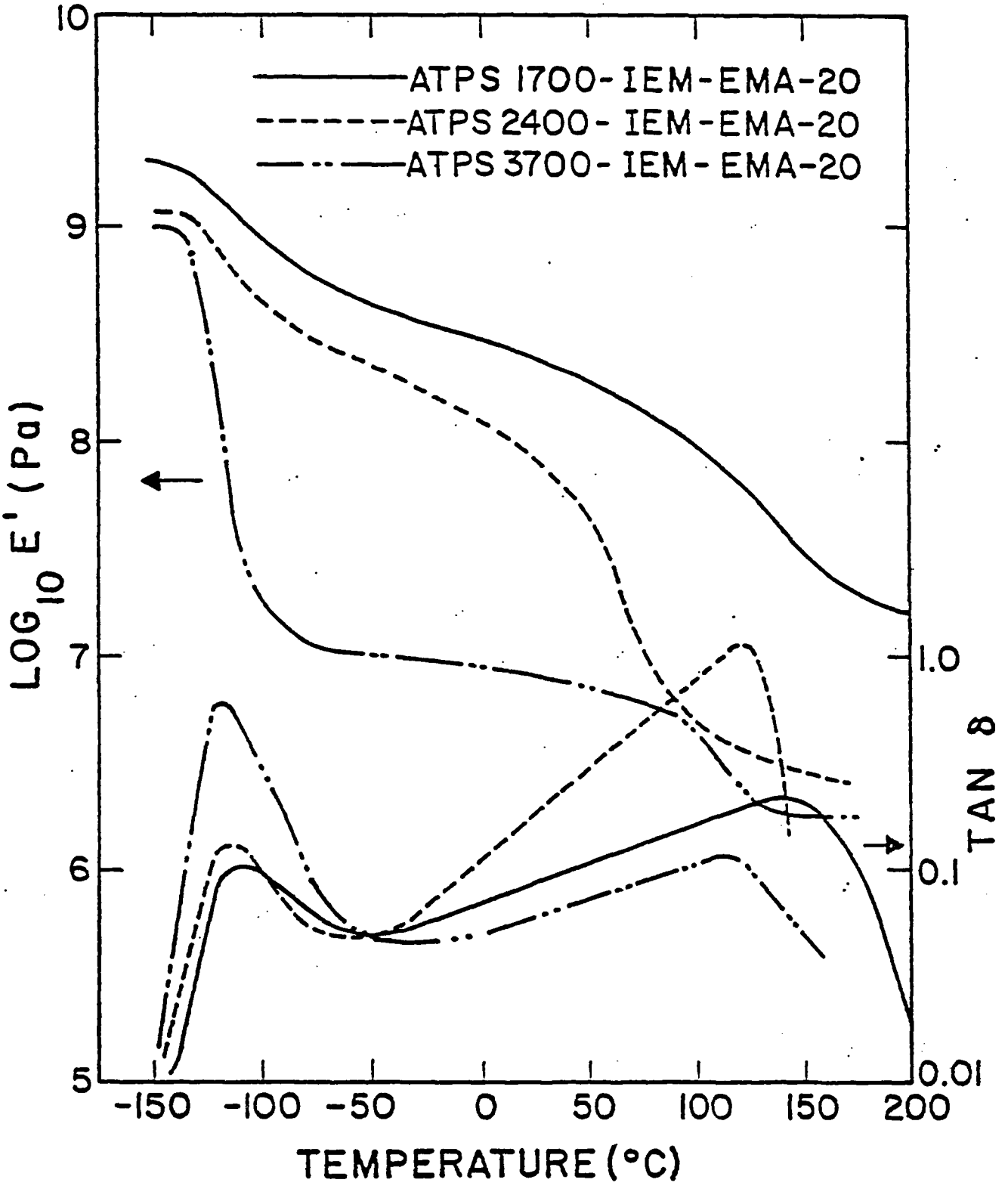
ATPS 1700-IEM-EMA-20
ATPS 2400-IEM-EMA-20
ATPS 3700-IEM-EMA-20
LOG10 E' (Pa)
TAN δ
TEMPERATURE (°C)
10
9
8
7
6
5
1.0
0.1
0.01
-150
-100
-50
0
50
100
150
200

FIGURE 8

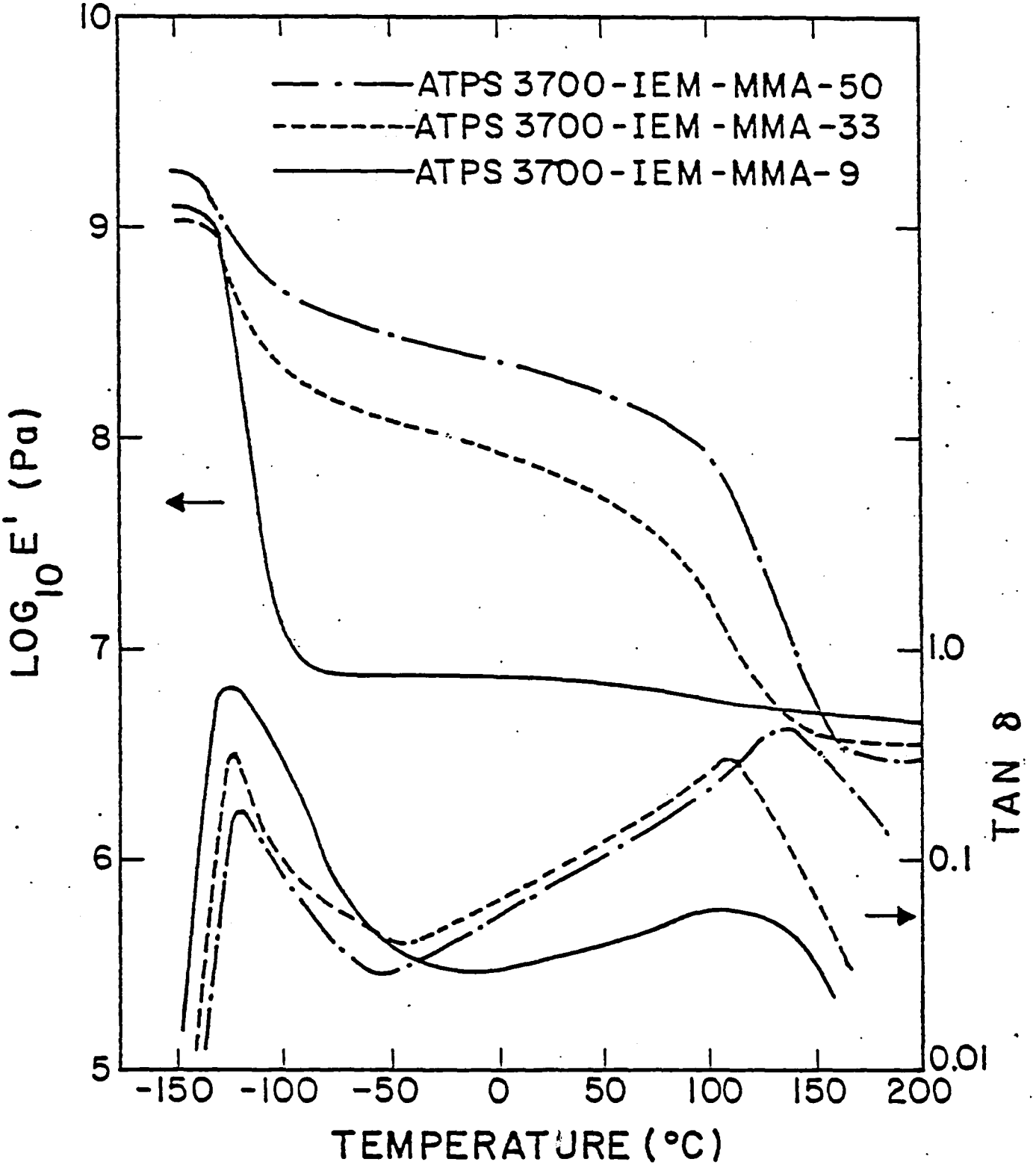
ATPS 3700-IEM-MMA-50
ATPS 3700-IEM-MMA-33
ATPS 3700-IEM-MMA-9
LOG10 E' (Pa)
TAN δ
TEMPERATURE (°C)
10
9
8
7
6
5
1.0
0.1
0.01
-150
-100
-50
0
50
100
150
200

FIGURE 9

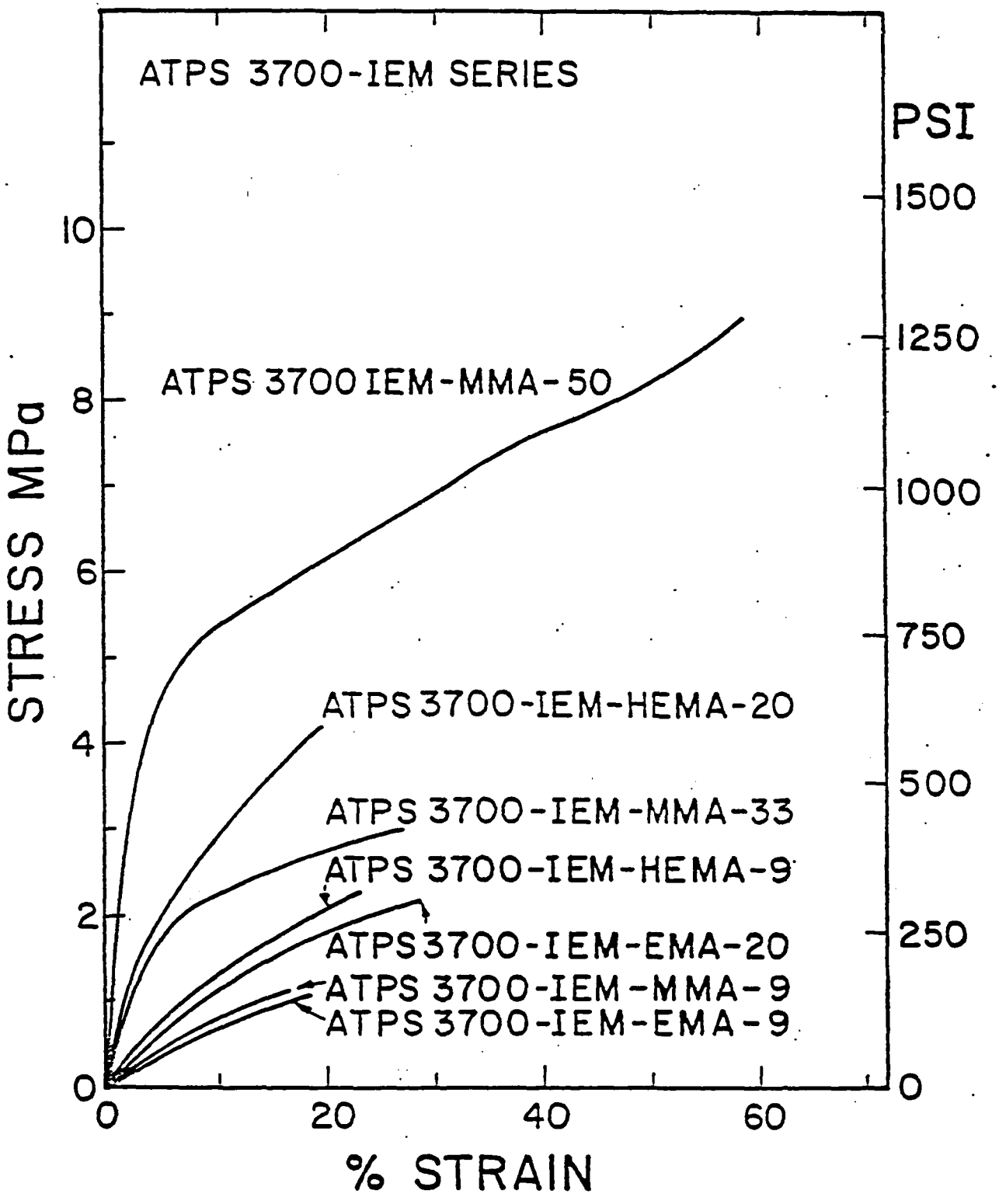
ATPS 3700-IEM SERIES
PSI
1500
1250
1000
750
500
250
0
10
8
6
4
2
0
STRESS MPa
ATPS 3700 IEM-MMA-50
ATPS 3700-IEM-HEMA-20
ATPS 3700-IEM-MMA-33
ATPS 3700-IEM-HEMA-9
ATPS3700-IEM-EMA-20
ATPS 3700-IEM-MMA-9
ATPS 3700-IEM-EMA-9
0
20
40
60
% STRAIN

FIGURE 10

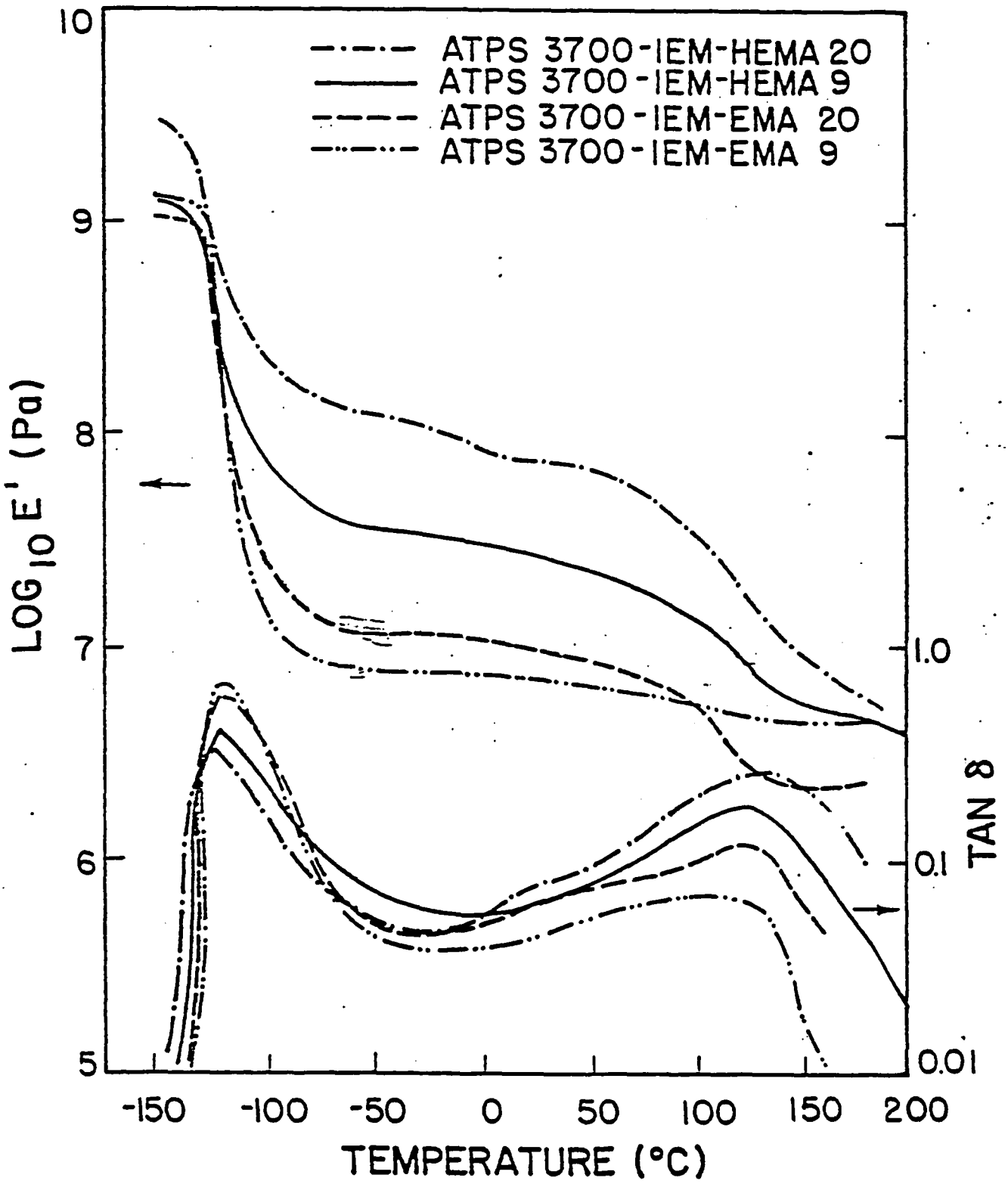
ATPS 3700-IEM-HEMA 20
ATPS 3700-IEM-HEMA 9
ATPS 3700-IEM-EMA 20
ATPS 3700-IEM-EMA 9
LOG10 E' (Pa)
TAN δ
TEMPERATURE (°C)
10
9
8
7
6
5
1.0
0.1
0.01
-150
-100
-50
0
50
100
150
200

FIGURE 11

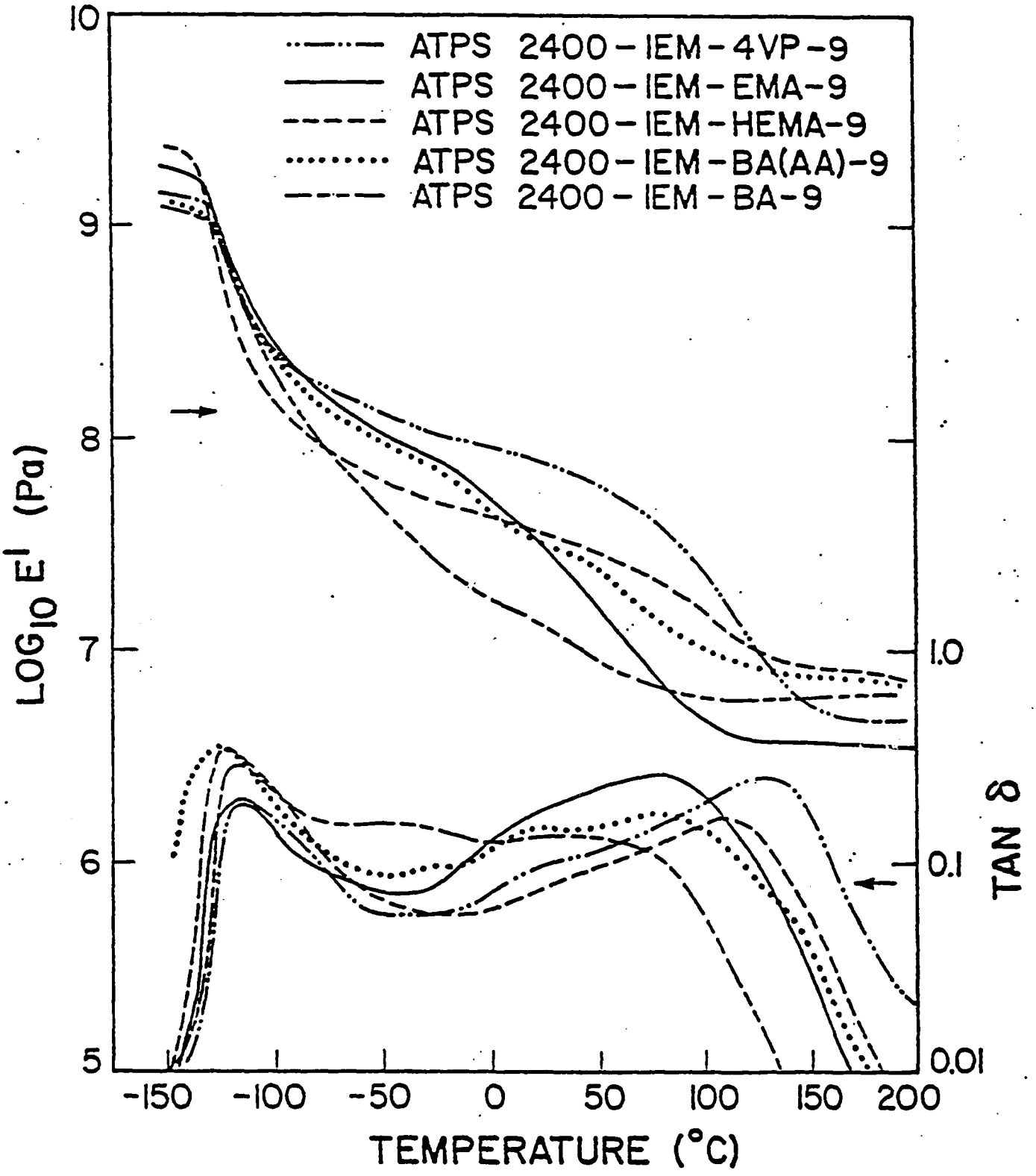
ATPS 2400-IEM-4VP-9
ATPS 2400-IEM-EMA-9
ATPS 2400-IEM-HEMA-9
ATPS 2400-IEM-BA(AA)-9
ATPS 2400-IEM-BA-9
LOG10 E' (Pa)
TAN δ
TEMPERATURE (°C)
10
9
8
7
6
5
1.0
0.1
0.01
-150
-100
-50
0
50
100
150
200

FIGURE 12

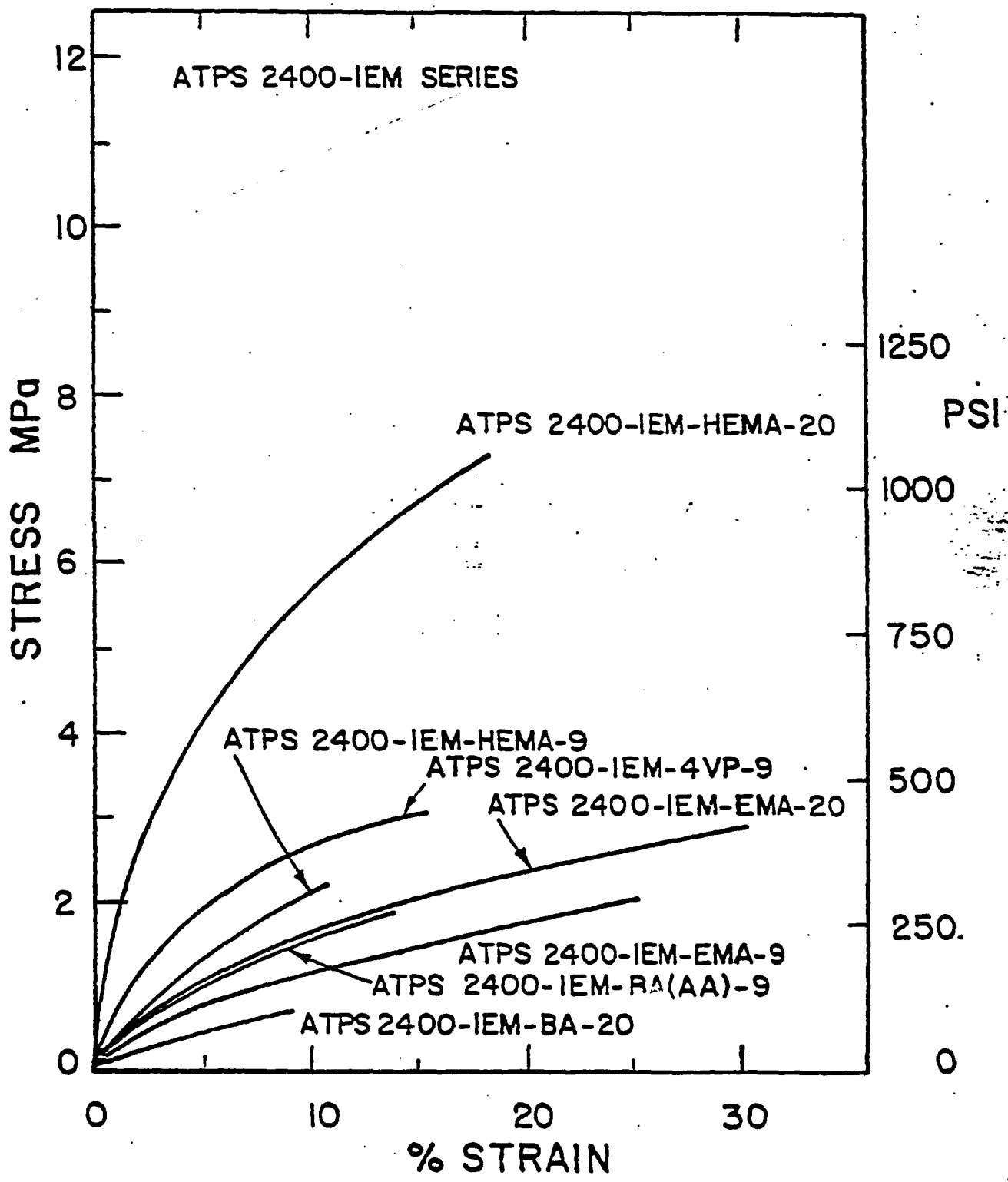
ATPS 2400-IEM SERIES
STRESS MPa
PSI
% STRAIN
0
2
4
6
8
10
12
0
10
20
30
250.
500
750
1000
1250
ATPS 2400-IEM-HEMA-20
ATPS 2400-IEM-HEMA-9
ATPS 2400-IEM-4VP-9
ATPS 2400-IEM-EMA-20
ATPS 2400-IEM-EMA-9
ATPS 2400-IEM-BA(AA)-9
ATPS 2400-IEM-BA-20

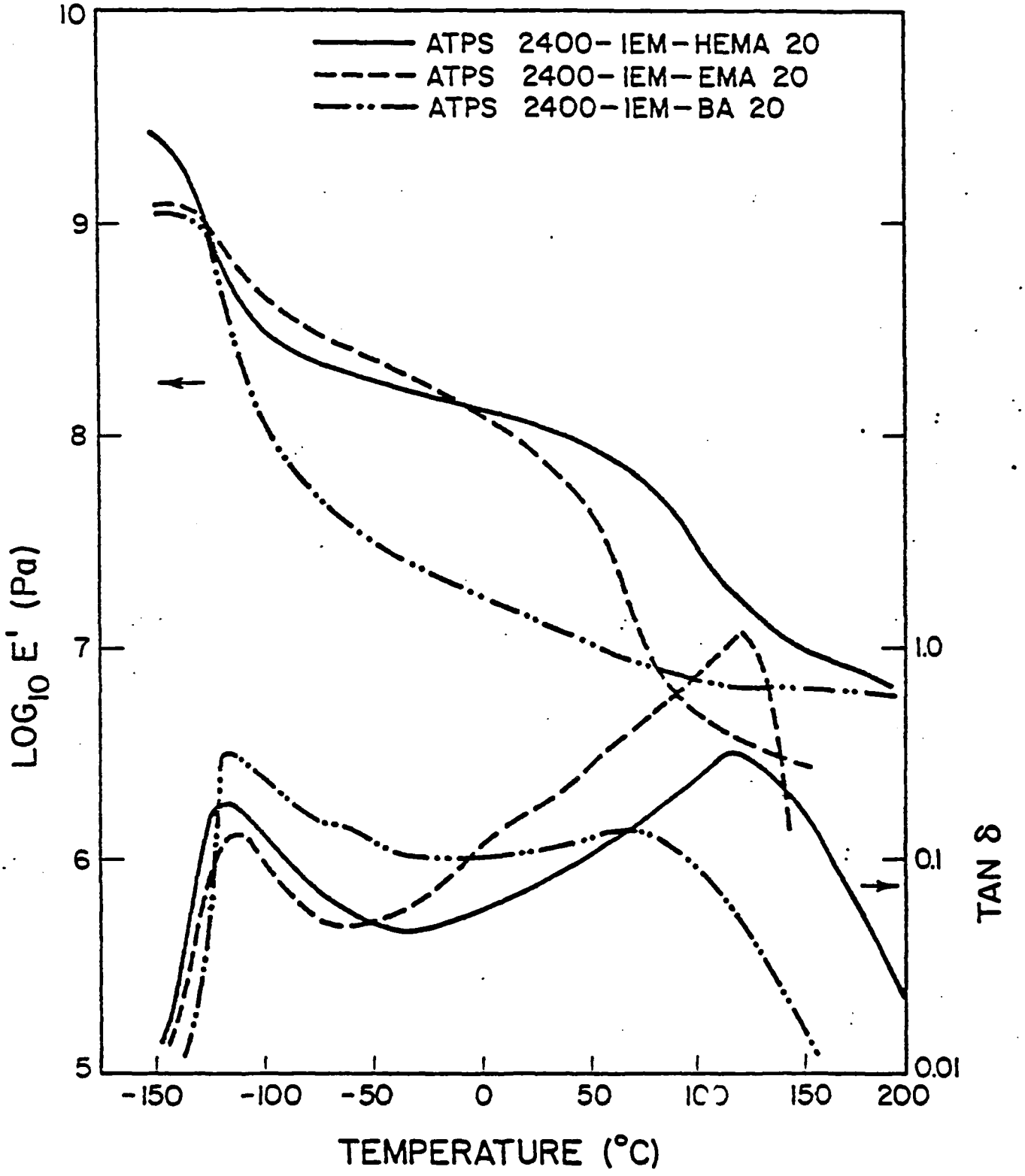
ATPS 2400-IEM-HEMA 20
ATPS 2400-IEM-EMA 20
ATPS 2400-IEM-BA 20
10
9
8
7
6
5
LOG10 E' (Pa)
1.0
0.1
0.01
TAN δ
-150
-100
-50
0
50
100
150
200
TEMPERATURE (°C)

FIGURE 14

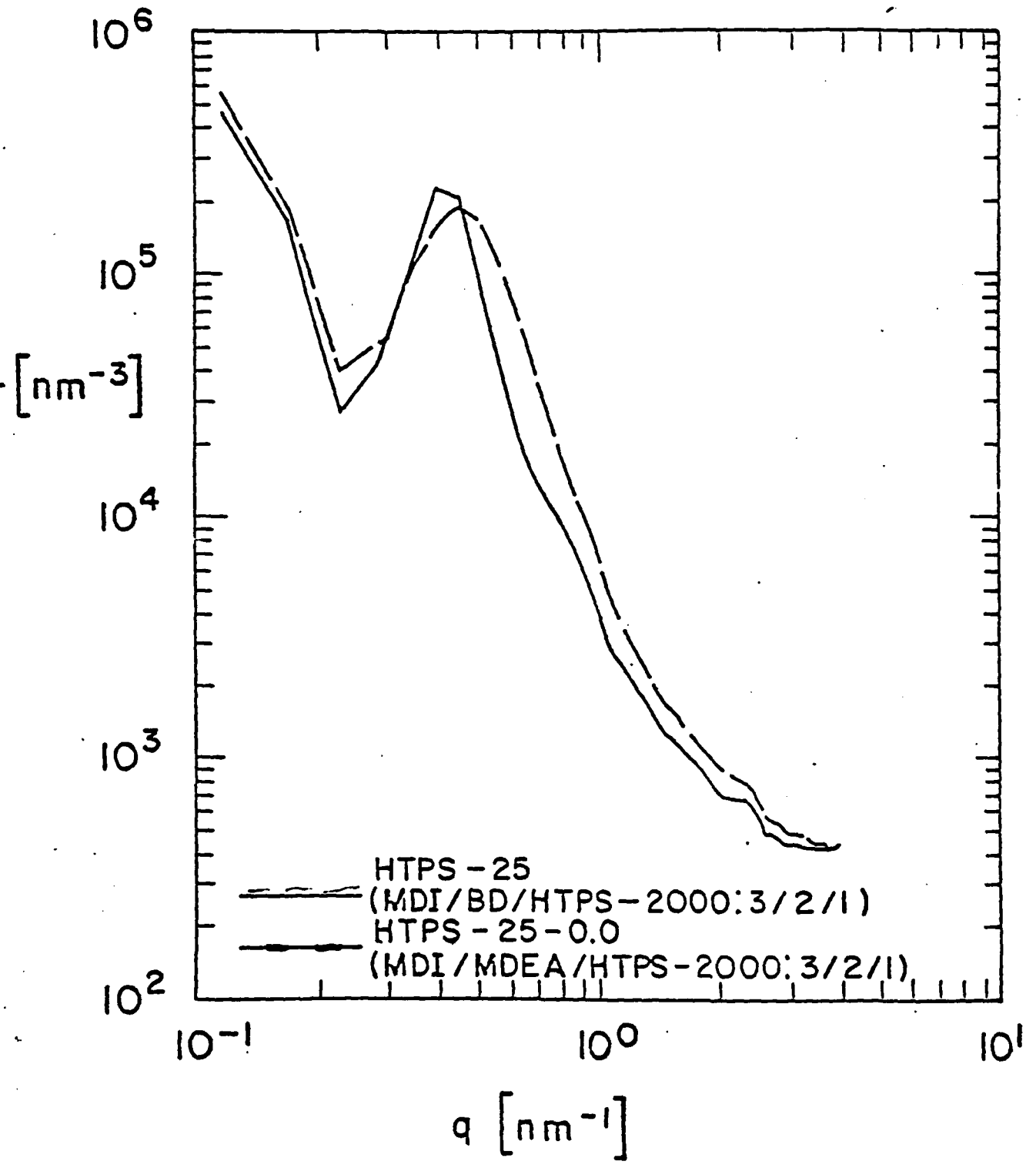
10^6
10^5
10^4
10^3
10^2
$\frac{I}{V}$ [nm^{-3}]
10^{-1}
10^0
10^1
q [nm^{-1}]
HTPS-25
(MDI/BD/HTPS-2000:3/2/1)
HTPS-25-0.0
(MDI/MDEA/HTPS-2000:3/2/1)

END

FILMED

1-85

DTIC